Article

In Situ Observation of Wetting and Drying of Montmorillonite in an Environmental Scanning Electron Microscope

J. Theo Kloprogge *

Posted Date: 28 February 2026

doi: 10.20944/preprints202602.1800.v1

Keywords: environmental scanning electron microscopy; montmorillonite; smectite; wetting cycle

doi:10.20944/preprints202602.1800.v1

Article

In Situ Observation of Wetting and Drying of Montmorillonite in an Environmental Scanning Electron Microscope

J. Theo Kloprogge

Department of Chemistry, College of Arts and Sciences, The University of the Philippines Visayas,
Miagao, 5023 Philippines; theoklop@bigpond.com

Abstract

Understanding the hydration dynamics of montmorillonite clay minerals is critical for predicting their behavior in geotechnical and environmental applications. This study employs in situ environmental scanning electron microscopy (ESEM) combined with X-ray diffraction (XRD) to directly observe and quantify the wetting and drying processes of montmorillonite SWy-1 under controlled pressure and temperature conditions. To characterize the real-time wetting and drying morphologies of montmorillonite and determine the relationship between water-induced swelling and relative humidity, ESEM enabled direct visualization of water-clay interactions by precisely controlling chamber pressure (4–5.3 Torr) and temperature (~2°C) to manipulate relative humidity and induce water condensation on mineral surfaces, while quantitative analysis of particle areas before and after hydration determined swelling percentages, XRD measured basal spacing (d_{001}) changes across relative humidity gradients, and water-adsorption isotherms were constructed from ESEM thickness measurements. ESEM revealed distinct wetting stages with water preferentially condensing on unsaturated edge sites and external surfaces at low pressures (<4.6 Torr), followed by rapid interlayer filling at elevated pressures with characteristic structural rounding and aggregate formation, while anisotropic swelling ocurred predominantly perpendicular to clay layers, with single water-layer hydration (1W) producing ~19% swelling and two-layer hydration (2W) yielding ~32% swelling, water-adsorption isotherms exhibited exponential swelling behavior with pronounced type H3 hysteresis, logarithmic analysis revealed steeper pressure dependency during hydration (slope = 2.7249) versus dehydration (slope = 1.6702) indicating thermodynamically driven water uptake but kinetically limited desorption, and rapid dehydration kinetics occurred within 3 minutes with complete equilibration by 15 minutes. ESEM successfully bridges microscale observations and molecular-scale understanding of smectite hydration, establishing practical timescales for clay equilibration and providing critical insights for predicting clay behavior in geotechnical engineering, soil stabilization, contaminant transport, and engineered barrier design.

Keywords: environmental scanning electron microscopy; montmorillonite; smectite; wetting cycle

1. Introduction

Smectites have been the focus of extensive scientific investigation over the years due to their intricate wetting and drying properties in different systems (e.g. [1–11]). The basic mechanisms for water interaction with these minerals need to be understood in order to describe the behavior of swelling clays in soils and predict their response to diferent environmental conditions. The interlayer distances in smectites are determined by two factors: water content in the interlayer space and the nature of balancing cations for layer charge. Important scientific contributions by researchers like Brindley and Brown [12], van der Gaast et al. [13,14], and other clay researchers [15–19] have shown that relative humidity has a direct effect on basal spacing in a stepwise manner.

doi:10.20944/preprints202602.1800.v1

The importance of the behavior of smectites far transcends purely theoretical soil science. In fact, in natural environments, water absorption by smectites in clays causes considerable swelling, and subsequent dehydration causes significant shrinkage—an effect that has serious consequences in practice. In Australia, for example, recent droughts have highlighted this effect in practice in a very significant way, resulting in considerable structural damage to residential buildings and infrastructure due to dehydration and subsequent rehydration of smectites in soils [20,21]. This is not an isolated incident; similar problems have been reported in a variety of geographical locations across the world due to problems with expanding clays [22–29]. In order to minimize construction and infrastructure risks, engineers must have a detailed understanding of the physical properties of expanding clays [30].

Apart from the issues of residential and civil engineering, the issues of expansive clays also relate to geomorphologic phenomena, including beach cliff erosion [3] and geological disposal of hazardous waste, where the integrity of clay barriers is of critical importance for the protection of the environment and public health [8,31,32]. To effectively address the complex issues of expansive clays, advanced characterization techniques are of critical importance. The ESEM, invented in the 1980s [33,34], represents a major technological advancement in the field of microscopy, where the use of wet, non-conductive samples is facilitated by the maintenance of a controlled environment in the microscope chamber. By adjusting the pressure and temperature of the microscope chamber, the relative humidity may be controlled by the condensation and evaporation of water vapor. Although this technique has been useful for the characterization of the behavior of clay minerals, its use for the characterization of smectite clay minerals has been restricted to a small number of studies [32,35–39].

This paper presents real-time in situ observations of montmorillonite wetting and drying using ESEM, documenting the changes in morphology and swelling behavior associated with variations in relative humidity caused by pressure and temperature adjustments.

2. Materials and Methods

For this research a very small amount of montmorillonite SWy-1 supplied by the Source Clay Repository of the Clay Minerals Society was added without any further pretreatment as a dry powder into a shallow holder specially made for the environmental electron microscope. Scanning electron microscope (SEM) images were obtained on a FEI Quanta 200 Environmental Scanning Electron Microscope (FEI Company, USA) operated at an accelerating voltage of 20 kV. The microscope was fitted with an FEI Peltier stage with a temperature controller and K-type thermocouple for monitoring the temperature. A gaseous secondary electron detector with a pressure limiting aperture, mounted directly above the specimen on the heating stage, was used for electron imaging. During the wetting and drying experiments, the detector-specimen distance was about 10mm. The specimen chamber pressure was adjusted according to the pressure and temperature diagram shown in Figure 1 around 5ºC and 4 to 6 Torr (water vapor). For digital image analysis the open source software, ImageJ, was used [40]. Montmorillonite aggregates with diameters between 30 and 50 mm were selected for area measurements. The selected ESEM images were converted to 8-bit and covered areas of 1024 pixels x 943 pixels. The area of interest (AOI) was isolated by applying a gray-level threshold. ImageJ considered a gray-level range of 0–255 for all area measurements. The increase in area was calculated from the following equation:

$$\text{Swelling (\%)} = ((A_h - A_0)/A_0)\text{x}100, \quad (1)$$

where A_h is the area (mm2) of the hydrated sample and A_0 is the initial area (mm^2) of the dry sample. The data are displayed as areal expansion (swelling %) vs. ESEM pressure in Torr at a fixed temperature and therefore can be indicated as isotherms. Hydration of the <1 μm size fraction of SWy-1 source clay (low-charge montmorillonite) was studied by modeling X-ray diffraction (XRD) patterns recorded under controlled relative humidity (RH) conditions. XRD patterns of the powdered samples were recorded on a Philips wide-angle PW1050/25 vertical goniometer applying Cu Kα radiation. The oriented clay samples were measured in step-scan mode with steps of 0.01 °2θ and a scan speed of 1.00° min-1 from 2°2θ to 20 °2θ to determine the value of d001

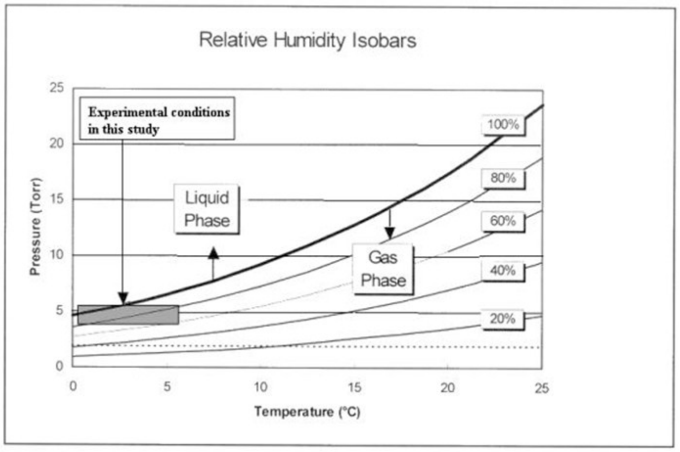

Figure 1. Pressure-temperature diagram of the water vapor-liquid transition.

3. Results

3.1. Wetting and Drying in the Environmental SEM

The ESEM results show the unique wetting/drying characteristics over three consecutive cycles, providing direct evidence for the water-clay interaction mechanisms previously characterized by other analytical methods. For the initial stage, the dry montmorillonite aggregates at 6°C, 5 Torr, quickly absorbed water after the pressure was increased to 6 Torr, forming large droplets within the clay particles, as shown in Figure 2. The quick wetting response is similar to the two-stage water hydration mechanism proposed in the molecular dynamic simulations on the montmorillonite hydration process [41]. The water absorption within the montmorillonite particles is attributed to the competitive hydration of the interlayer sites, which was confirmed by the quantitative hydration study on montmorillonite hydration, where the difference in water uptake within the interlayer and on the surface is characterized by thermogravimetric analysis and nuclear magnetic resonance spectroscopy [42]. These results are also consistent with the earlier ESEM study on the hydration characteristics of clay minerals under controlled humidity conditions, confirming the validity of the experimental approach.

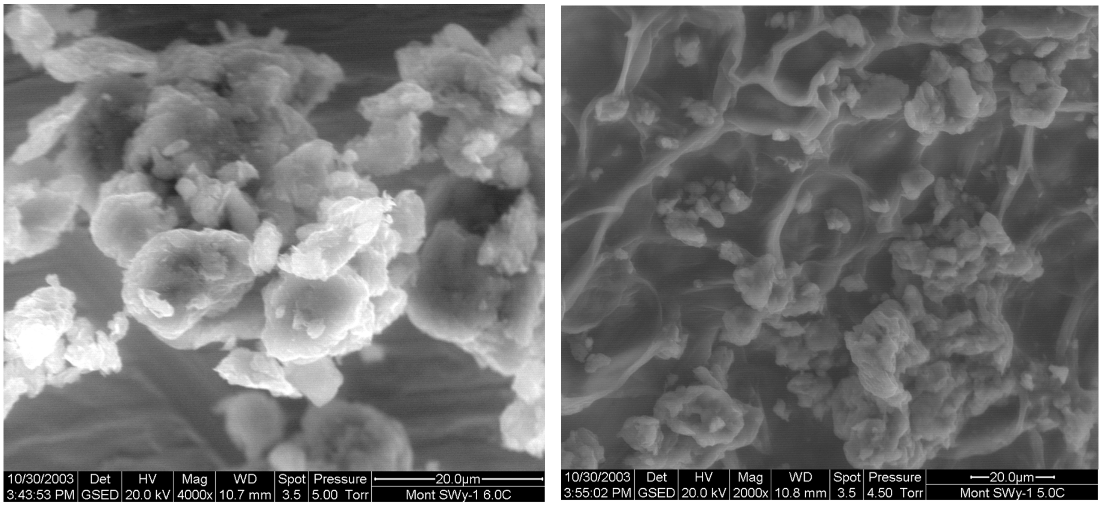

(**a**) (**b**)

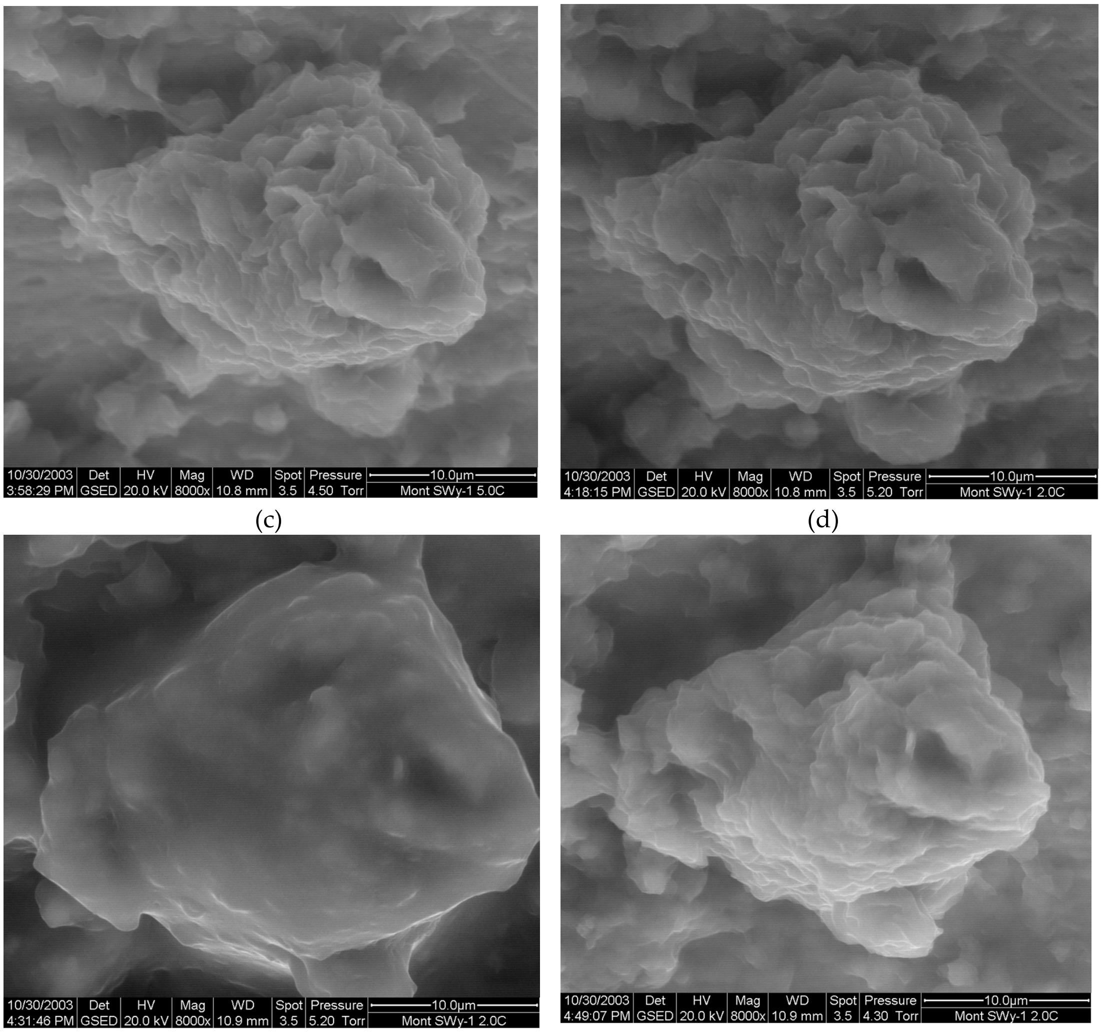

(c) (d)

(e) (f)

Figure 2. Environmental SEM images under various pressure and temperature conditions (**a**) Dry montmorillonite before wetting at 4.5 Torr and 5 °C; (**b**) Formation of rounded rims of montmorillonite clay after the vast evaporation of water droplets at 4.5 Torr and 5 °C; (**c**). Dry aggregate after the first wetting and drying cycle (4.5 Torr, 5 °C); (**d**) Montmorillonite is still dry after cooling to 2 °C at 5.2 Torr; (**e**) Montmorillonite aggregate completely wetted at 5.2 Torr and 2 °C; and (**f**) Montmorillonite aggregate after drying (4.3 Torr, 2 °C).

The subsequent cooling to 5°C at 4.5 Torr caused rapid water evaporation, concentrating the montmorillonite on the periphery of the droplets, producing the typical features of rounded, elevated rims on the sample holder. This is evidence of the dynamic nature of water loss in the interlayer space. The open, porous morphology caused by the rapid water evaporation, as observed in the second cycle, is similar to the morphologies described in the SEM studies on smectites (e.g. [43,44]). Recent ESEM examinations on oriented montmorillonite clay films, where the effects of humidity-induced swelling/drying were monitored by digital image correlation and related to the changes in the interlayer spacing determined by X-ray diffraction [36], offer direct visual evidence for the effects of rapid dehydration, which is in line with the theoretical predictions on hydration-driven phase transitions [45].

The second cycle of wetting and drying provided critical mechanistic insights into the selective hydration process. With incremental increases in pressure to 5.2 Torr, subtle edge rounding was observed (Figure 3), suggesting selective water condensation onto charged edge sites as opposed to hydrophobic 001 basal faces—a characteristic feature ascribed to hydroxyl groups from unsaturated Al and Si bonds at particle edges. This selective edge hydration is also predicted by molecular simulation studies of the hydration dynamic processes for sodium montmorillonite hydration, where it is predicted that water molecules prefer to form hydrogen bonds with bridging oxygen atoms and surface hydroxyl groups prior to interlayer hydration [45]. The critical aspect is that interlayer hydration was observed upon a subsequent increase in pressure to 5.3 Torr, confirming the presence of hydration thresholds as predicted by stepwise crystalline swelling transitions in molecular simulation studies of montmorillonite hydration with varying cations. These transitions are characteristic of established 0W (0 water layers), 1W (1 water layer), and 2W (2 water layers) hydration states as established in classical studies of montmorillonite hydration [12–14]. The presence of open morphologies following drying cycles, as observed in the third cycle, is also consistent with studies of wetting/drying hysteresis in clay minerals, where mechanical changes to pore structures are also observed to accumulate over cycling.

The above observations collectively confirm the two-step mechanism of montmorillonite wetting: slow water condensation on the edges of the montmorillonite particles at lower pressures due to hydroxyl group interaction, followed by rapid hydration between the interlayers upon exceeding a critical pressure threshold. The pressure dependence of the wetting process, along with the changes in the montmorillonite structure, can be related to the thermodynamic properties of confined water in clay minerals. The two-step mechanism of montmorillonite wetting has been confirmed by molecular dynamic simulations, which show the thermodynamic barriers and interfacial phase transitions in the transition from a particular hydration state to another, for instance, from a 1-water configuration to a 2-water configuration in the interlayer space of the montmorillonite particles [46]. The semi-logarithmic dependence of the hydration/dehydration isotherms confirms the existence of two different mechanisms of montmorillonite wetting. The large difference in the slopes of the hydration and dehydration isotherms (hydration: 2.7249, R^2: 0.9756, dehydration: 1.6702, R^2: 0.9967) emphasizes the different nature of the two mechanisms. The wetting mechanisms of montmorillonite have been interpreted in different ways in the literature. Fu et al. [16] attribute the environmental effects impeding the desorption process to the decrease in entropy. In contrast, the geometrical factors, including the arrangement of particles and changes in the interlayer spacing, are highlighted in the study of Cases et al. [47]. The study of Tompsett et al. [48] reveals the potential of network effects and cavitation phenomena in the explanation of the large hysteresis loops in the wetting/drying process of montmorillonite particles, which can be confirmed by Monte Carlo simulations. The dynamic character of the wetting process of montmorillonite particles, the changes in the structure of the montmorillonite particles upon wetting, and the presence of the morphological signs of the drying cycles of the montmorillonite particles provide a real-time visual image of the interaction of the montmorillonite particles with water. The wetting/drying process of montmorillonite particles can be related to the hysteresis loops in the gas adsorption/desorption process.

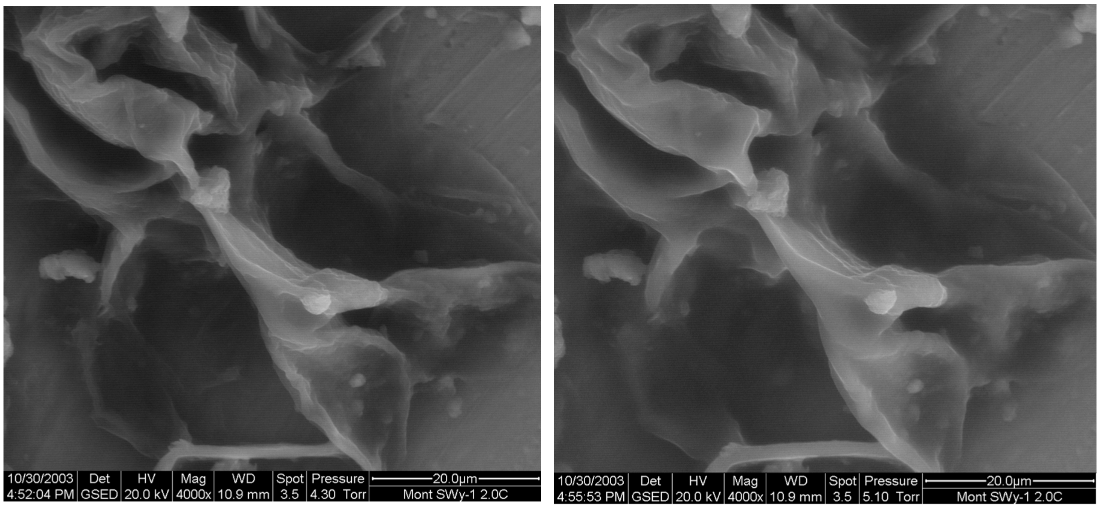

(**a**) (**b**)

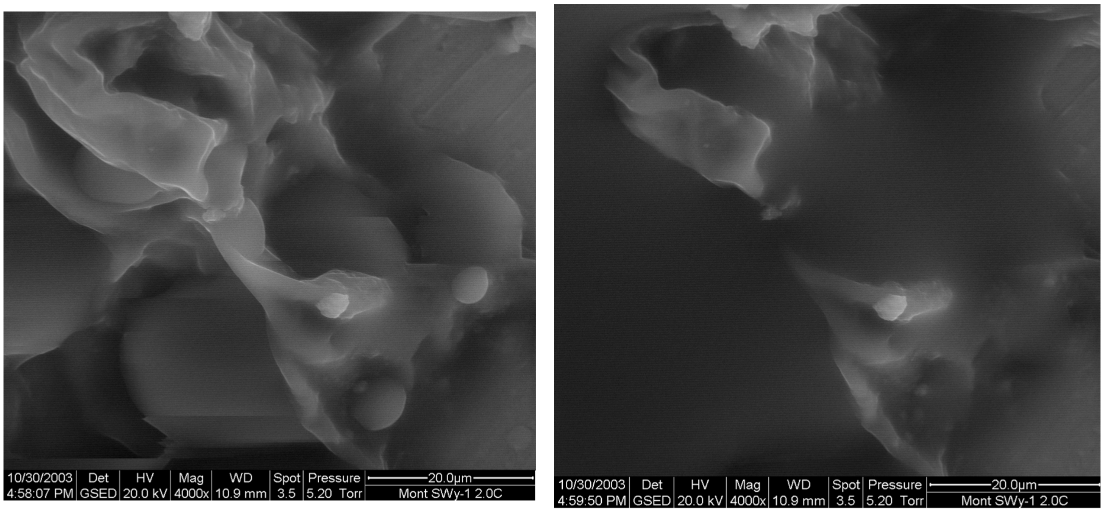

(c) (d)

Figure 3. Environmental SEM images under various pressure and temperature conditions (**a**) Close up of one of the rims shown in Figure 2(**b**) at 4.3 Torr and 2 °C; (**b**) Increased pressure to 5.1 Torr resulted in a rounding of the edges of the montmorillonite particles; (**c**). Increased wetting of the montmorillonite after increasing the pressure to 5.2 Torr at 2 °C; (**d**) Complete wetting has taken place 103 seconds after the image shown in Figure 3(**c**) was taken (5.2 Torr and 2 °C).

3.2. Swelling and Drying as Function of Relative Humidity Inside XRD

In order to confirm the observations made from the ESEM analysis, X-ray diffraction analysis was carried out at different levels of relative humidity. X-ray diffraction analysis is a robust technique for the analysis of the behavior of clay minerals. The technique provides information on the basal d-spacing (d_{001}) of clay minerals, which directly corresponds to the distance between successive clay layers in the interlayer region. The measurement of the basal d-spacing is sensitive to the presence of water molecules in the interlayer region of the clay minerals. Therefore, the X-ray diffraction technique can provide information on the changes in the structure of swelling clay minerals during the sorption/desorption of moisture [49].

The investigation of water vapor adsorption/desorption in smectite clay has provided significant evidence of the systematic increase in interlayer spacing. This is an indication of the existence of various hydration states with zero, one, or two water layers in the interlayer spaces of smectite clay minerals [50]. Figure 4 shows that the swelling of the SWy-1 montmorillonite clay upon an increase in relative humidity is reflected in the XRD results. In the results, the typical hydration states were observed: the 0W state with a d_{001} spacing of 9.6 to 10.1 Å at 0% RH, the 1W state with a d_{001} spacing of 12.3 to 12.7 Å, and the 2W state with a d_{001} spacing of 15.0 to 15.8 Å (e.g. [12,13,15,47,51–54]). These hydration states are associated with specific basal spacing driven by the number of water molecule layers present in the interlayer spaces of the clay. These states are controlled by the balance of water-clay electrostatic interactions and osmotic pressures of the interlayer solution [55]. The presence of interlayer exchangeable cations has a significant effect on the swelling of clay minerals as well as the transitions of hydration states [50]. Na^{+}-saturated montmorillonite has more swelling compared to Ca^{2+}-saturated montmorillonite.

XRD analysis indicates significant hysteresis between wetting and drying processes due to kinetic limitations in water movement between layers and differences in thermodynamic stability [49]. Significantly, intermediate relative humidity ranges exhibit the coexistence of different hydration states, characterized by basal spacings between discrete values (0W, 1W, 2W). This phenomenon of interstratification points to spatial heterogeneity in hydration states within the clay aggregate; that is, different parts or domains in the aggregate may have different hydration states at a given relative humidity.

The XRD d-spacing values also correlate with ESEM observations (Section 3.1), offering a multi-scale view of water penetration into clay aggregates. Figure 4 shows the link between nanometer-scale d-spacing variations and the resulting micrometer-scale aggregate morphological variations observed by ESEM. The stepwise hydration transitions are important for modeling mechanical properties, permeability, and contaminant flow in clay-rich media. The 1W to 2W transition involves a large d-spacing increase from 12.5 Å to 15.4 Å (Figure 4), which is critical for mechanical compliance and flow. Interestingly, the reversibility of these transitions during drying cycles and hysteretic behavior also generate "memory effects" in mechanical and hydraulic properties as a function of wetting/drying history, a significant factor for long-term behavior of clay barriers and foundations.

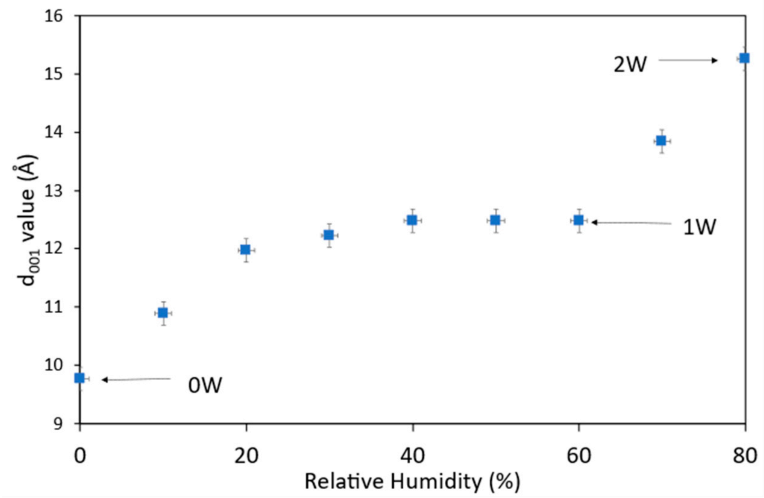

Figure 4. Variations of the basal spacing d001 of montmorillonite SWy-1 measured on experimental XRD patterns as a function of relative humidity. W = water layer.

3.3. Water Adsorption Isotherms Based on ESEM Thickness Measurements

The swelling tendency of smectite-type clays, i.e., montmorillonite, is mainly along the c-axis. Quantitative evaluation of this phenomenon is possible by measuring the dimensions of the ac and bc planes before and after the hydration process, thereby facilitating the calculation of the swelling percentage. Based on the assumed geometrical parameters, it is expected that the addition of one water layer, i.e., 1W, will cause an increase in the area by 16%, whereas the addition of two water layers, i.e., 2W, will cause the area to increase by 32%. It is interesting to note that these theoretical evaluations show good correlation with the experimental results, where the swelling percentage is found to be 19% and 32%, respectively, for the addition of one and two water layers. The anisotropic swelling characteristics are typical for the considered clay minerals, i.e., those with layered structures, which have been well demonstrated in the ESEM study on thin clay films, where the c-axis expansion is dominant, whereas the other dimensions are relatively unchanged [36].

To determine the kinetics of dehydration in montmorillonite SWy-1, it was necessary to set the initial pressure level to 5.3 Torr for a 10-minute equilibration time. After this equilibration period, the pressure level was reduced to 4.3 Torr to commence the dehydration process. Montmorillonite was observed to exhibit a rapid release of adsorbed water molecules, leading to a significant reduction in swelling. In this case, swelling was reduced to 3% in just 3 minutes. However, it was possible to regain the original dimension in approximately 10 minutes. This indicates that a 15-minute duration is adequate to ensure equilibrium conditions are met. This is a clear indication that montmorillonite is a complex compound that binds water molecules in a complex manner. In this case, it is clear that loosely bound water molecules are released rapidly. However, it is also clear that tightly bound water molecules, as is the case in inner-sphere complexes around interlayer cations, require a longer time to be released [49]. This duration is deemed adequate to enable a comprehensive analysis of montmorillonite's hydrophilic characteristics by conducting subsequent water adsorption isotherm measurements.

The water adsorption isotherm for montmorillonite SWy-1 at 2°C (Figure 5a) indicates a multi-regime swelling response characteristic of expansive clay minerals. The rates of swelling are low during hydration as a result of a greater tendency for water to condense on the surface of particles and edges, where unsaturated bonds are present for adsorption. It is interesting to note that differentiation in particle morphologies is evident only upon application of a pressure of 5.2. This indicates a threshold pressure level beyond which hydration is thermodynamically feasible. Beyond a threshold pressure level of 4.6, there is an exponential relationship between swelling pressure and swelling percentage. This is indicative of a change to a multilayer hydration mechanism. The exponential relationship between swelling pressure and swelling percentage is indicative of a cumulative effect as a result of interlayer hydration. This is also indicative of a cooperative effect between water molecules as they are adsorbed into interlayer spaces [50]. Conversely, there are marginally elevated swelling percentages as a result of a reduction in pressure.

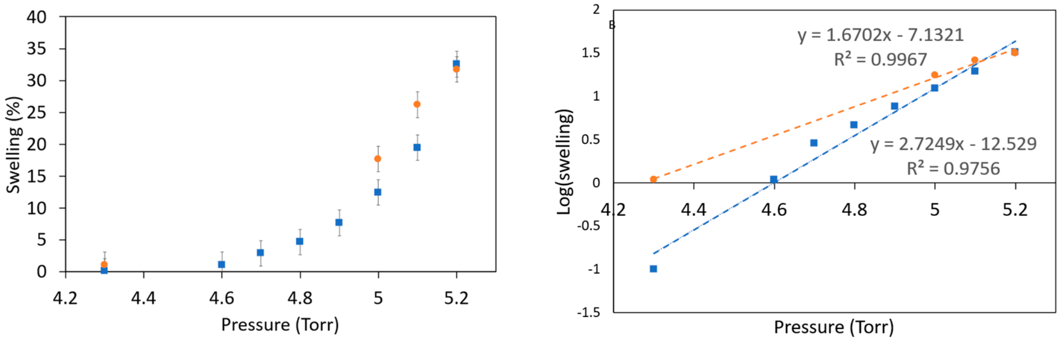

(**a**) (**b**)

Figure 5. (**a**) Measured isotherms of montmorillonite SWy-1 at 2°C. Filled squares: hydration path; filled circles: dehydration path; (**b**) Semi-logarithmic plot of swelling vs. pressure representing a first-order reaction of the hydration process with hindered dehydration (t_{equil} = 15 min).

The observed hysteresis behavior is consistent with gas adsorption isotherm behavior as reported in gas adsorption studies, specifically those employing the Brunauer-Emmett-Teller (BET) method for smectite clay minerals. The observed hysteresis loop in the experiment corresponds to type H3, characteristic of plate-like particles that form slit-shaped pores as previously reported [56]. A logarithmic analysis of the swelling isotherm according to pressure shows a linear behavior for the hydration cycle, as represented by a slope value of 2.7249 (R^2 value = 0.9756). This is unlike the dehydration cycle, where a slope value of 1.6702 (R^2 value = 0.9967) is observed, thereby showing a greater pressure dependency. The greater slope value for hydration indicates that hydration is controlled by thermodynamic forces such as the electrostatic attraction between the negatively charged surface and polar water molecules. In contrast, the lower slope value for dehydration suggests that it is controlled by kinetics such as diffusion through tortuous paths and the strength of hydrogen bonds between water molecules and clay surfaces [55].

The difference in slope also reinforces the uniqueness of the swelling mechanism. This finding is supported by past studies; however, there are varying opinions. For example, Fu, Zhang, and Low [16] explain that the environmental conditions that impede desorption are a result of a reduction in entropy as a result of thermodynamic ordering of interlayer molecules as they form extensive hydrogen-bond networks. Cases et al. [47], on the other hand, have focused their explanations on geometric considerations such as variations in particle arrangement and spacing that result in tortuous paths for water molecules to diffuse into the interlayer spaces and reduce molecular mobility in confined spaces. Recent studies have established that the initial hydration status of smectite minerals, whether dry or prehydrated, affects the pathways and mechanism by which subsequent water molecules are bound [57]. Tompsett et al. [48] have also suggested that network effects and cavitation could be used to explain the wide hysteresis loops observed in mesoporous materials by employing a Monte Carlo method. It is also possible that all these processes have varying contributions to the overall swelling mechanism based on the type of clay material used, type of interlayer cations, and humidity levels used in such studies.

In conclusion, the water adsorption isotherms for montmorillonite SWy-1 depicted in Figure 5a show complex thermodynamic and kinetic phenomena involving various ranges of pressure and humidity. The water adsorption isotherms obtained experimentally show that there is minimal initial swelling of the clay mineral at low pressures, exponential swelling at intermediate pressures, and significant hysteresis in the wetting-drying isotherms. These water adsorption isotherms obtained experimentally match very well with the current understanding of the hydration of smectite clay minerals obtained using molecular dynamics simulation and thermodynamic modeling, which show that there is a dynamic equilibrium of water in the interlayer spaces of clay minerals due to opposing forces of attraction to the surface of the clay mineral and entropy due to ordering of molecules in the interlayer spaces. These phenomena explain the memory effect of clay minerals in which the mechanical and hydraulic properties of clay minerals depend on the history of wetting-drying cycles. These phenomena are very important in understanding the behavior of clay minerals in various applications from geotechnical engineering to environmental remediation and development of advanced clay-based composites.

4. Conclusions

The current study elucidated the efficacy of environmental scanning electron microscopy (ESEM), an effective methodology, in the study of the wetting and drying dynamics of mineral specimens, with an emphasis on smectite minerals, such as montmorillonite SWy-1. The ability to precisely control the pressure and temperature within the sample environment empowers the researcher to manipulate the relative humidity and condense water directly onto the mineral specimen. The controlled environment will permit the real-time study of the wetting and drying dynamics of the montmorillonite specimen, thus allowing for a better comprehension of the swelling and wetting properties of the mineral, as well as the formation of various aggregates, as observed in the traditional scanning electron microscopy (SEM).

The measurements carried out in this study show a marked anisotropic swelling behavior of montmorillonite SWy-1, where the material swells mainly in the direction perpendicular to the stacking of the clay particles. This is a crucial observation because it highlights the directional characteristics of the material's swelling. This can have a substantial influence on the physical characteristics of the material in different geological or engineering situations. In addition, the hydration isotherm for montmorillonite SWy-1 shows an exponential relationship, implying a substantial increase in the material's swelling at high pressures. These observations are crucial in the advancement of the theoretical framework of the behavior of clay minerals. They help in the formulation of precise prediction models for the performance of the material in different situations in the fields of soil science, geotechnical engineering, environmental science, and so forth.

To conclude, apart from contributing to the knowledge of the dynamics of montmorillonite in the presence of moisture, this study also adds credence to the application of the ESEM method in mineralogy. The real-time observation capabilities that are inherent in this method are capable of providing unprecedented insights into the complex interplay between moisture and clay minerals, thus leading to further exploration of their consequences.

Funding: This research received no external funding.

Data Availability Statement: Data is contained within the article.

Acknowledgments: The author thanks the School of Chemistry, Physics, and Mechanical Engineering, QUT, Brisbane, for the use of the ESEM and XRD for this study.

Conflicts of Interest: The author declares no conflicts of interest.

Abbreviations

The following abbreviations are used in this manuscript:

SWy-1	Montmorillonite
ESEMJ	Environmental Scanning Electron Microscopy
XRD	X-ray Diffraction
AOI	Area of interest
RH	Relative Humidity
A_h	Area of hydrated sample
A_0	Initial area of dry sample

References

1. Aylmore, L.A.G.; Quirk, J.P. Swelling of Clay–Water Systems. *Nature* **1959**, *183*, 1752-1753. 10.1038/1831752a0.
2. Blackmore, A.V.; Miller, R.D. Tactoid Size and Osmotic Swelling in Calcium Montmorillonite. *Soil Science Society of America Journal* **1961**, *25*, 169-173. 10.2136/sssaj1961.03615995002500030009x.
3. Diop, S.; Ogawa, Y.; Zhang, M. Effects of Cyclic Wetting and Drying on Physical and Mechanical Properties of Neogene Sandstones and Siltstones from Boso Peninsula, Japan. *Jour. Japan Soc. Eng. Geol.* **2008**, *49*, 150-163.
4. Gillott, J.E. Chapter 6 - Moisture Interaction with Clays and Clay Minerals. In *Developments in Geotechnical Engineering*, Gillott, J.E., Ed.; Elsevier: 1987; Volume 41, pp. 167-217.
5. Güven, N.; Pollastro, R.M. *Clay-water interface and its rheological implications*; The Clay Minerals Society: Boulder, 1992; Volume 4, p. 244.
6. Newman, A.C.D. The significance of clays in agriculture and soils. *Philosophical Transactions Royal Society, London* **1984**, *A 311*, 375-389.
7. Newman, A.C.D. The interaction of water with clay mineral surfaces. In *Chemistry of clays and clay minerals*, Newman, A.C.D., Ed.; Longman Scientific & Technical: Harlow, 1987; pp. 237-274.
8. Pusch, R.; Nakano, M.; Yong, R.N.; Yang, T. Long-term function of on-ground repositories for hazardous waste - Mechanisms in cyclic drying/wetting of top clay liners. *Journal of Earth Sciences and Geotechnical Engineering* **2017**, *7*, 45-62.
9. Shahsavani, S.; Vakili, A.H.; Mokhberi, M. The effect of wetting and drying cycles on the swelling-shrinkage behavior of the expansive soils improved by nanosilica and industrial waste. *Bulletin of Engineering Geology and the Environment* **2020**. 10.1007/s10064-020-01851-6.
10. Taylor, R.K.; Smith, T.J. The engineering geology of clay minerals: swelling, shrinking and mudrock breakdown. *Clay Minerals* **1986**, *21*, 235-260. 10.1180/claymin.1986.021.3.01.
11. Wang, B.-t.; Zhang, C.-h.; Qiu, X.-l.; Ji, E.-y.; Zhang, W.-h. Research on Wetting-Drying Cycles' Effect on the Physical and Mechanical Properties of Expansive Soil Improved by OTAC-KCl. *Advances in Materials Science and Engineering* **2015**, *2015*, 304276, 304271-304277. 10.1155/2015/304276.
12. Brindley, G.W.; Brown, G. Crystal Structures of Clay Minerals and their X-ray Identification; Mineralogical Society: London, 1984.
13. Kuhnel, R.A.; van der Gaast, S.J. Humidity controlled diffractometry and its applications. *Advances in X-Ray Analysis* **1993**, *36*, 439-449.
14. Van der Gaast, S.J.; Kuhnel, R.A.; Vasterink, J.; Frost, R.L. A new model for the structure of water in the interlayer of Ca-Wyoming montmorillonite. *Clays Our Future, Proc. Int. Clay Conf., 11th* **1997**, 421-427.
15. Ferrage, E. Investigation of smectite hydration properties by modeling experimental X-ray diffraction patterns: Part I. Montmorillonite hydration properties. *American Mineralogist* **2005**, *90*, 1358-1374. 10.2138/am.2005.1776.

16. Fu, M.H.; Zhang, Z.Z.; Low, P.F. Changes in the Properties of a Montmorillonite-Water System during the Adsorption and Desorption of Water: Hysteresis1. *Clays and Clay Minerals* **1990**, *38*, 485-492. 10.1346/ccmn.1990.0380504.
17. Morida, K.; Fukushi, K.; Sakuma, H.; Tamura, K. Systematic comparison of the hydration and dehydration of Na+-, K+-, and NH4+-saturated montmorillonite, nontronite, hectorite, saponite, and Fe-saponite by in situ X-ray diffraction measurements. *Applied Clay Science* **2023**, *237*, 106898. https://doi.org/10.1016/j.clay.2023.106898.
18. Morodome, S.; Kawamura, K. In situ X-ray diffraction study of the swelling of montmorillonite as affected by exchangeable cations and temperature. *Clays and Clay Minerals* **2011**, *59*, 165-175. 10.1346/CCMN.2011.0590205.
19. Tamura, K.; Yamada, H.; Nakazawa, H. Stepwise hydration of high-quality synthetic smectite with various cations. *Clays and Clay Minerals* **2000**, *48*, 400-404. 10.1346/CCMN.2000.0480311.
20. Al-Taie, A.; Disfani, M.M.; Evans, R.; Arulrajah, A.; Horpibulsuk, S. Swell-shrink Cycles of Lime Stabilized Expansive Subgrade. *Procedia Engineering* **2016**, *143*, 615-622. 10.1016/j.proeng.2016.06.083.
21. Vanorio, T. Elastic properties of dry clay mineral aggregates, suspensions and sandstones. *Geophysical Journal International* **2003**, *155*, 319-329. 10.1046/j.1365-246X.2003.02046.x.
22. Apriyono, A.; Yuliana, Y.; Kamchoom, V.; Leung, A.K.; Jotisankasa, A. The effects of desiccation crack and seasonal variation on hydrological response of compact clay embankment. *Canadian Geotechnical Journal* **2025**, *62*, 1-16. 10.1139/cgj-2024-0570.
23. Chittoori, B.C.S.; Puppala, A.J.; Pedarla, A. Addressing Clay Mineralogy Effects on Performance of Chemically Stabilized Expansive Soils Subjected to Seasonal Wetting and Drying. *Journal of Geotechnical and Geoenvironmental Engineering* **2018**, *144*, 04017097. 10.1061/(asce)gt.1943-5606.0001796.
24. Kalantari, B. Engineering significant of swelling soils. *Research Journal of Applied Sciences, Engineering and Technology* **2012**, *4*, 2874-2878.
25. Kumar, A.; Biswas, N.; Puppala, A.J.; Mebarkia, B. Forensic investigation and chemical remediation of a collapsed highway embankment slope in Houston, Texas. *Transportation Geotechnics* **2025**, *51*, 101503. 10.1016/j.trgeo.2025.101503.
26. Liu, W.; Tan, J.; Wu, J.; Xu, L.; Wan, J. Effect of cyclic wetting on lateritic clay subgrade settlement and train-track dynamic response of high-speed railway. *Transportation Geotechnics* **2025**, *51*, 101541. 10.1016/j.trgeo.2025.101541.
27. Shah, S.S.A.; Turrakheil, K.S.; Naveed, M. Impact of Wetting and Drying Cycles on the Hydromechanical Properties of Soil and Implications on Slope Stability. *Atmosphere* **2024**, *15*, 1368. 10.3390/atmos15111368.
28. Walker, C.; Heitor, A.; Clarke, B.G. Impact of drying-wetting cycles on the small strain behaviour of compacted clay. *Transportation Geotechnics* **2023**, *42*, 101063. 10.1016/j.trgeo.2023.101063.
29. Zemenu, G.; Martine, A.; Roger, C. Analysis of the behaviour of a natural expansive soil under cyclic drying and wetting. *Bulletin of Engineering Geology and the Environment* **2009**, *68*, 421-436. 10.1007/s10064-009-0203-4.
30. Totsche, K.U. Microaggregates in soils. *Journal of Plant Nutrition and Soil Science* **2017**, *180*, 15-21. 10.1002/jpln.201600451.
31. Al-Mahbashi, A.M.; Al-Shamrani, M.A.; Abbas, M.F. Hydromechanical behavior of unsaturated expansive clay under repetitive loading. *Journal of Rock Mechanics and Geotechnical Engineering* **2021**, *13*, 1136-1146. 10.1016/j.jrmge.2021.05.002.
32. Montes-H, G. Swelling–shrinkage measurements of bentonite using coupled environmental scanning electron microscopy and digital image analysis. *Journal of Colloid and Interface Science* **2005**, *284*, 271-277. 10.1016/j.jcis.2004.09.025.
33. Danilatos, G.D. Foundations of environmental scanning electron microscopy. *Advances in Electronics and Electronic Physics* **1988**, *71*, 109-250.
34. Danilatos, G.D. Introduction to the ESEM instrument. *Microscopy Research and Technique* **1993**, *25*, 354-361.
35. Baker, J.C.; Grabowska-Olszewska, B.; Uwins, P.J.R. ESEM study of osmotic swelling of bentonite from Radzionkow (Poland). *Applied Clay Science* **1995**, *9*, 465-469.
36. Carrier, B.; Wang, L.; Vandamme, M.; Pellenq, R.J.M.; Bornert, M.; Tanguy, A.; Van Damme, H. ESEM Study of the Humidity-Induced Swelling of Clay Film. *Langmuir* **2013**, *29*, 12823-12833. 10.1021/la402781p.

doi:10.20944/preprints202602.1800.v1

37. Friedrich, F.; Schild, D.; Weidler, P.G.; Schäfer, T.; Schäfer, T.; Dohrmann, R.; Greenwell, H.C. Hydration of Febex Bentonite as Observed by Environmental Scanning Electron Microscopy (ESEM). In *Filling the Gaps – from Microscopic Pore Structures to Transport Properties in Shales*; Clay Minerals Society: 2016; Volume 21, p. 0.
38. Kloprogge, J.T.; Duong, L.V.; Frost, R.L.; Boström, T.L. Use of environmental scanning electron microscopy to study uncoated minerals. *Microscopy and Analysis* **2005**, *19*, 17–19.
39. Romero, E.; Simms, P.H. Microstructure Investigation in Unsaturated Soils: A Review with Special Attention to Contribution of Mercury Intrusion Porosimetry and Environmental Scanning Electron Microscopy. *Geotechnical and Geological Engineering* **2008**, *26*, 705-727. 10.1007/s10706-008-9204-5.
40. Schneider, C.A.; Rasband, W.S.; Eliceiri, K.W. NIH Image to ImageJ: 25 years of image analysis. *Nature Methods* **2012**, *9*, 671-675. 10.1038/nmeth.2089.
41. Chen, L.; Wu, Z.; Xu, L.; Li, Z.; Zhang, Y.; Xia, W. Hydration-Driven Interfacial Behaviors of Nanoconfined Sodium Montmorillonite. *Langmuir* **2025**, *41*, 31471-31480. 10.1021/acs.langmuir.5c04534.
42. Xie, G.; Xiao, Y.; Deng, M.; Zhang, Q.; Huang, D.; Jiang, L.; Yang, Y.; Luo, P. Quantitative Investigation of the Hydration Behavior of Sodium Montmorillonite by Thermogravimetric Analysis and Low-Field Nuclear Magnetic Resonance. *Energy & Fuels* **2019**, *33*, 7483-7492. 10.1021/acs.energyfuels.9b01170.
43. Tessier, D.; Pedro, G. Electron microscopy study of Na smectite fabric - role of layer charge, salt concentration and suction parameters. In *Developments in Sedimentology*, van Olphen, H., Veniale, F., Eds.; Elsevier: Amsterdam, 1982; Volume 35, pp. 165-176.
44. Tessier, D.L.A.; Petit, J.C. Relation between macroscopic behavior of clays and their microstructural. *Applied Geochemistry* **1992**, Suppl. Issue 1, 151-161.
45. Teng, Y.; Chen, C.; Zheng, L.; Whittaker, M.L. Optically Triggered Nucleation Eliminates Hydration Hysteresis in Swelling Minerals. *Langmuir* **2025**, *41*, 11307-11313. 10.1021/acs.langmuir.4c04468.
46. Teng, F. Optically Triggered Nucleation Eliminates Hydration Hysteresis in Swelling Minerals. *Langmuir* **2025**. 10.1021/acs.langmuir.4c04468.
47. Cases, J.M.; Berend, I.; Besson, G.; Francois, M.; Uriot, J.P.; Thomas, F.; Poirier, J.E. Mechanism of adsorption and desorption of water vapor by homoionic montmorillonite. 1. The sodium-exchanged form. *Langmuir* **1992**, *8*, 2730-2739. 10.1021/la00047a025.
48. Tompsett, G.A.; Krogh, L.; Griffin, D.W.; Conner, W.C. Hysteresis and Scanning Behavior of Mesoporous Molecular Sieves. *Langmuir* **2005**, *21*, 8214-8225. 10.1021/la050068y.
49. Nair, A.K.N.; Cui, R.; Sun, S. Overview of the Adsorption and Transport Properties of Water, Ions, Carbon Dioxide, and Methane in Swelling Clays. *American Chemical Society* **2021**. 10.1021/acsearthspacechem.1c00160.
50. Zhang, W.; Chen, S.; Tong, K.; Li, S.; Huang, K.; Dai, Z.; Luo, L. Effects of the Layer Charge Location and Interlayer Cation on Rectorite Swelling Properties: Comparison between Molecular Dynamics Simulations and Experiments. *American Chemical Society* **2022**. 10.1021/acs.jpcc.2c02549.
51. Emmerich, K.; Koeniger, F.; Kaden, H.; Thissen, P. Microscopic structure and properties of discrete water layer in Na-exchanged montmorillonite. *Journal of Colloid and Interface Science* **2015**, *448*, 24-31. 10.1016/j.jcis.2015.01.087.
52. Hetzel, F. The Microstructure of Three NA+ Smectites: The Importance of Particle Geometry on Dehydration and Rehydration. *Clays and Clay Minerals* **1994**, *42*, 242-248. 10.1346/ccmn.1994.0420302.
53. Saiyouri, N.; Tessier, D.; Hicher, P.Y. Experimental study of swelling in unsaturated compacted clays. *Clay Minerals* **2004**, *39*, 469-479. 10.1180/0009855043940148.
54. Sato, T.; Watanabe, T.; Otsuka, R. Effects of layer charge, charge location, and energy change on expansion properties of dioctahedral smectites. *Clays and Clay Minerals* **1992**, *40*, 103–113.
55. Endo, M.; Sato, H. Swelling Stress of Bentonite: Thermodynamics of Interlayer Water in K-Montmorillonite in Consideration of Alteration. *Minerals* **2024**. 10.3390/min14040430.

56. Xiong, Q.; Baychev, T.G.; Jivkov, A.P. Review of pore network modelling of porous media: Experimental characterisations, network constructions and applications to reactive transport. *Journal of Contaminant Hydrology* **2016)**, *192*, 101-117. https://doi.org/https://doi.org/10.1016/j.jconhyd.2016.07.002.
57. Prastistho, W.; Apsari, C.N.; Gusnaniar, N.; Budianta, W.; Promentilla, M.; Utami, S.T. Re-evaluating the evidence of aflatoxin B1 intercalation into smectite interlayer: a review based on basal spacing data. *Sains Tanah: Journal of Soil Science and Agroclimatology* **2025**. 10.20961/stjssa.v22i1.92453.